Interchain coherence of coupled Luttinger liquids at all orders in perturbation theory

Enrico Arrigoni
Institut für Theoretische Physik, Universität Würzburg, D-97074 Würzburg, Germany

We analyze the problem of Luttinger liquids coupled via a single-particle hopping $t_\perp$ and introduce a systematic diagrammatic expansion in powers of $t_\perp$. An analysis of the scaling of the diagrams at each order allows us to determine the power-law behavior versus $t_\perp$ of the interchain hopping and of the Fermi surface warp. In particular, for strong interactions, we find that the exponents are dominated by higher-order diagrams producing an enhanced coherence and a failure of linear-response theory. Our results are valid at any finite order in $t_\perp$ for the self-energy.

PACS numbers : 71.10.Pm, 71.10.Hf, 05.30.Fk, 71.15.-m, **to appear in Phys. Rev. Lett.**

The problem of crossover from one to higher dimensions has recently received particular interest [1–9]. The puzzling question is whether and how an infinite row of one-dimensional chains of Luttinger liquids (LL) develops interchain coherence and possibly goes over into a Fermi-liquid state for an arbitrarily weak single-particle hopping $t_\perp \ll E_F$ between the chains (E_F being the Fermi energy), and how this is affected by the correlation exponent α [10] of the unperturbed LL which parametrizes the *intrachain* interaction. No clear agreement has been reached so far and different analyses have provided conflicting answers: (i) The system might go over to a Fermi-liquid state for arbitrarily small $t_\perp$, or (ii) there might be a finite $t_\perp$ (depending on α) below which the systems remains in a LL state and no coherence is developed between the liquids [6], or finally (iii) one could have a different state possibly with gaps and long-range order. This ambiguity is essentially due to the fact that the perturbation introduced by $t_\perp$ is *relevant* [3–5]. This means that no matter how small $t_\perp$, perturbative results in $t_\perp$ will be always inaccurate for sufficiently low values of some characteristic energy $\mathcal{E} \lesssim \mathcal{E}_0 = (t_\perp/E_F^\alpha)^{1/(1-\alpha)}$. Here, $\mathcal{E}$ is the largest energy scale between (i) the external frequency ω, (ii) the momentum measured from the Fermi surface $|k-k_F|$ [10], and (iii) the temperature T. Indeed, in the interesting region $\mathcal{E} \sim \mathcal{E}_0$, where interchain coherence starts to set on [5], all perturbation terms are of the same order and no definitive prediction can be made about the nature of the ground state. An alternative approach to this topic is to consider the limit of strong forward scattering where one can use the higher-dimensional bosonization method [7] or the Ward identities [4]. In this limit, one can show that a system always becomes a Fermi liquid in dimensions greater than one if the interaction is not too singular.

In this Letter, we analyze how *interchain coherence* develops when $t_\perp$ is switched on and its α dependence. The striking point of the present work is that the results are valid at *any finite order* in $t_\perp$ for the single-particle self-energy, in contrast to previous work [2,5,6,8]. This is important because it fixes some essentially exact results to which approximate theories should be compared, although it is clear that an answer to the more interesting question "Fermi liquid or not" *to this degree of accuracy* is extremely difficult and will not be addressed here. In addition, we show that restricting to lowest-order terms may give incorrect results even in the small $t_\perp$ limit for α larger than a certain value. In particular, when considering higher-order diagrams, interchain coherence is increased, and linear-response theory does not work. Specifically, we evaluate the exponent of the power-law behavior in $t_\perp$ (i) of the interchain hopping of a particle at the Fermi momentum, and (ii) of the Fermi surface (FS) warp. To calculate these quantities we extend a method developed in Ref. [11] to the case of coupled LL and rewrite diagrammatically the perturbation expansion in $t_\perp$ introduced in Ref. [5]. We then consider the low-energy scaling behavior of the diagrams at all orders in $t_\perp$ and notice that the scaling is no longer homogeneous for $\alpha > \alpha_{2p}$ (cf. also Refs. [9,5]). Finally, we use this scaling behavior to calculate the exponents mentioned above. Recent exact-diagonalization calculations [12] are in excellent agreement with our predictions.

We consider a system of N coplanar coupled identical chains lying parallel to the x-axis with Hamiltonian $H = \sum_i H_{LL}(i) + \sum_{ijr\sigma} t_{\perp ij} \int dx \;\; \psi^\dagger_{r,\sigma}(x;i)\psi_{r,\sigma}(x;j)$, where $H_{LL}(i)$ describes a (uncoupled) Luttinger liquid in chain i, $t_{\perp ij}$ is a hopping term between chain i and j, and $\psi_{r,\sigma}(x;i)$ ($\psi^\dagger_{r,\sigma}(x;i)$) is the destruction (creation) operator for a right- ($r=+1$) or left-moving ($r=-1$) fermion at site x in the chain i with spin σ (we will also consider the spinless case). The diagrammatic expansion in t around the atomic limit of the Hubbard model introduced by W. Metzner in Ref. [11] can be readily extended to the present case by considering perturbations in $t_\perp$ about the exactly-solvable Hamiltonian for the isolated Luttinger liquids $\sum_i H_{LL}(i)$. We consider the diagrammatic expansion for the Green's function $\mathcal{G}(k_\parallel, i\omega; k_\perp)$ expressed in the imaginary-frequency ($i\omega$) and momentum representation, where $k_\parallel$ and $k_\perp$ label the Fourier transforms of the x and of the i components, respectively. Unless otherwise specified, $k_\parallel$ will also implicitly contain the other in-chain quantum numbers r and σ. The expansion of $\mathcal{G}(k_\parallel, i\omega; k_\perp)$ in $t_\perp$ is obtained by drawing all connected diagrams composed of two external lines, and of an arbitrary number of vertices connected with directed lines, each vertex having a number of entering lines equal to the number of leaving lines (see Fig. 1).

One then labels each internal line (l) by a momentum (${k_\parallel}^{(l)}$, ${k_\perp}^{(l)}$) and a frequency variable ($i\omega^{(l)}$), and the external lines by $k_\parallel$, $k_\perp$ and $i\omega$. Each *internal* line (l) yields a factor $t_\perp[{k_\perp}^{(l)}]$ (the Fourier transform of $t_{\perp ij}$). Each vertex with $2n$ legs ($2n \geq 2$) acquires a contribution $C_n^0({k_\parallel}^{(1)} i\omega^{(1)}, \cdots {k_\parallel}^{(n)} i\omega^{(n)} | {k_\parallel}^{(1)\prime} i\omega^{(1)\prime}, \cdots {k_\parallel}^{(n)\prime} i\omega^{(n)\prime})$, where C_n^0 is the n-particle cumulant of the isolated chain (for example, $C_2^0 = \mathcal{G}^0$, the LL Green's function), and ${k_\parallel}^{(l)} i\omega^{(l)}$, ${k_\parallel}^{(l)\prime} i\omega^{(l)\prime}$ are the frequency and momenta (which are conserved at the vertex) of the entering and leaving lines, respectively (cf. [11,5]). The introduction of higher-order cumulants and vertices is necessary, since the correlation functions of the $t_\perp = 0$ Hamiltonian do not satisfy Wick's theorem. Eventually, one has to multiply each diagram by the usual symmetry and fermion factors and integrate (or sum) over all internal frequencies and momenta. This is a diagrammatic representation of the expansion introduced by D. Boies and coworkers in Ref. [5]. Similarly to conventional diagrammatic theory (cf. also Ref. [11]), one can introduce a "self-energy" $\Gamma(k_\parallel, i\omega; k_\perp)^{-1}$. The "inverse-self-energy" $\Gamma(k_\parallel, i\omega; k_\perp)$ is then obtained by summing all one-particle-irreducible contributions to $\mathcal{G}(k_\parallel, i\omega; k_\perp)$ (see Fig. 1c). One then obtains an analogue of the Dyson equation (cf. Fig. 1b): $\mathcal{G}(k_\parallel, i\omega; k_\perp) = \left(\Gamma(k_\parallel, i\omega; k_\perp)^{-1} - t_\perp[k_\perp]\right)^{-1}$.

At this point, it is clear that the approximation used in Refs. [2,5,6,8] (and others) consists in considering only the contribution to Γ from the first diagram (the dot α) in Fig. 1(c) ["single-dot" approximation (SDA)] and thus using $\Gamma = \mathcal{G}^0$. Furthermore, one can obtain the limit of infinite coordination $D \to \infty$ by summing an infinite series of "bow" diagrams with "full" self-consistent Green's functions as internal lines (cf. Ref. [11]). Nevertheless, we briefly review the results obtained by others [2,5,8] within this SDA. Here, the system (both spinless and spinful) *behaves as a Fermi liquid* for any values of the correlation exponent $\alpha < 1$ [10], in the sense that there is a warped (i. e., $k_\perp$-dependent) FS ${k_\parallel}_F[k_\perp]$, on which the Green's function has a (real) pole with finite weight at $\omega = 0$ and there is a *finite* region in momentum space around ${k_\parallel}_F[k_\perp]$ where the pole survives, remains real, and continuously shifts to higher binding energies [13]. The quasiparticles are thus well defined everywhere on the FS (except at the *special* points for which $t_\perp[k_\perp] = 0$). Other poles [6] do not describe true quasiparticles, since their imaginary part is always of the same order as their energy.

However, the trouble starts to arise when one tries to consider higher-order diagrams. A simple power-counting argument indeed shows that a diagram of order ${t_\perp}^{n-1}$ for Γ diverges like $E_F^{-n\alpha}\mathcal{E}^{n(\alpha-1)}$ in the low-$\mathcal{E}$ limit. If one tries to keep the *effective expansion parameter* $t_\perp E_F^{-\alpha}\mathcal{E}^{\alpha-1}$ small, then the $t_\perp[k_\perp]$ term in the denominator of $\mathcal{G}(k_\parallel, i\omega; k_\perp)$ becomes much smaller than $\Gamma(k_\parallel, i\omega; k_\perp)^{-1}$ and the system behaves as a sum of uncoupled LL. On the other hand, as soon as one tries to approach the pole, the approximation fails and higher-order diagrams become of the same order of magnitude. For this reason, nothing reliable can be said about possible Fermi-liquid behavior at this order of perturbation and it is mandatory to consider higher-order diagrams. In addition, the above power-counting argument does not hold for all values of α. For α greater than a certain α_{2p} some diagrams turn out to diverge stronger at low frequencies (cf. also Refs. [9,3,5]). For example, the contribution to $t_\perp\Gamma(\mathbf{x}_1 - \mathbf{x}_2; k_\perp)$ [14] from the diagram γ (Fig. 1c), with internal lines $3, 4, 5$ taking the r indices $+, -, -$, respectively, is proportional to [15]

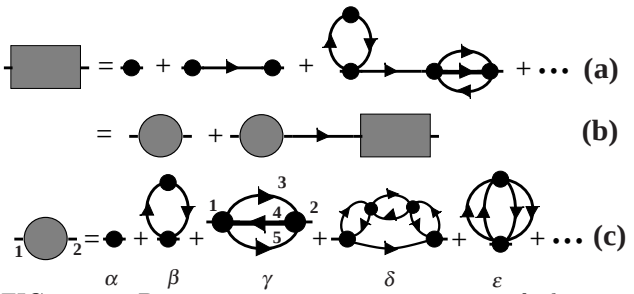

FIG. 1. Diagrammatic expansion in $t_\perp$ of the single-particle Green's function $\mathcal{G}$ (gray box). Directed lines give a contribution $t_\perp[k_\perp]$, and a dot with n entering and n leaving lines contributes a factor C_n^0 (n-particle cumulant). (a) Example of single-particle irreducible and reducible contributions to $\mathcal{G}$. (b) Dyson's equation for $\mathcal{G}$ in terms of the inverse-self-energy Γ (gray disk). (c) Example of diagrams contributing to Γ (some of them are discussed in the text).

$$\left(\frac{t_\perp}{E_F^\alpha}\right)^4 \cos k_\perp \int \prod_{i=3}^{5} d^2\mathbf{x}_i \ \left(|\mathbf{x}_1 - \mathbf{x}_3|\,|\mathbf{x}_4 - \mathbf{x}_5|\right)^{-1-\alpha} \times \left[\left(\frac{|\mathbf{x}_1 - \mathbf{x}_5|\,|\mathbf{x}_3 - \mathbf{x}_4|}{|\mathbf{x}_1 - \mathbf{x}_4|\,|\mathbf{x}_3 - \mathbf{x}_5|}\right)^{-B} - 1\right] \times e^{-i(\arg(\mathbf{x}_1 - \mathbf{x}_3) - \arg(\mathbf{x}_4 - \mathbf{x}_5))} \times (\text{term with } \mathbf{x}_1 \to \mathbf{x}_2)\ , \tag{1}$$

where $|\mathbf{x}| \equiv \sqrt{x^2 + (|\tau| + a)^2}$, $\arg \mathbf{x} \equiv \arg(x + i\tau)$, and the exponent $B = (1/K_\rho - K_\rho)/(2S)$. A naive dimensional analysis yields a term $\propto \left(t_\perp/E_F^\alpha\right)^4 |\mathbf{x}_1 - \mathbf{x}_2|^{2-4\alpha}$, giving a contribution proportional to $\left(t_\perp/(E_F^\alpha \mathcal{E}^{1-\alpha})\right)^4$ to the Fourier transform $t_\perp\Gamma(k_\parallel, i\omega; k_\perp)$. This is correct for $\mathcal{E} \ll E_F$ if the integral does not diverge at small distances for $a \to 0$, i.e. as long as $B < 1$. For $B > 1$ [10] one picks up an a-dependent contribution $a^{2-2B} \sim E_F^{2B-2}$, which must be balanced by $\mathcal{E}^{2-2B}$ to give the correct energy dimensions. This produces a contribution to $t_\perp\Gamma(k_\parallel, i\omega; k_\perp)$ proportional to $\left(t_\perp/(E_F^\alpha \mathcal{E}^{1-\alpha})\right)^4 (E_F/\mathcal{E})^{2B-2}$, i.e. a stronger divergence. A similar analysis shows that the 7-legs diagram δ in Fig. 1(c) and its generalizations with $2n + 1$ internal legs (n odd integer) produce a contribution to $t_\perp\Gamma$ proportional to $\left(t_\perp/(E_F^\alpha \mathcal{E}^{1-\alpha})\right)^{2n+2} (E_F/\mathcal{E})^{2n(B-1)}$. In fact, this is the strongest low-energy divergence one can attain for a contribution to $t_\perp\Gamma$ at a given order

${t_\perp}^{2n+2}$. The regime $B > 1$ corresponds to $\alpha > \alpha_{2p}$ with $\alpha_{2p} = (\sqrt{S^2+1}-1)/S$, i.e., where two-particle processes become more relevant than one-particle processes [5,9].

We now use the above results to calculate the power-law behavior for small $t_\perp$ of the quantity [14]

$$\Delta n_{k_F} \propto \int_{-\infty}^{\infty} d\omega \left[\mathcal{G}(k_F, i\omega; \pi) - \mathcal{G}(k_F, i\omega; 0)\right] . \quad (2)$$

Δn_{k_F} is also equal to the expectation value of the single-particle hopping operator at k_F in the two-chains case and is thus a measure of the *coherence* [6] of single-particle hopping. For $k = k_F$ and $T = 0$ the only remaining energy scale that can be associated with $\mathcal{E}$ is ω. For $\alpha < \alpha_{2p}$ all diagrams scale in the same way as discussed above. Therefore, *at any order in the $t_\perp$ expansion* and for $\omega \ll E_F$ the difference between the Green's function of the two bands $\mathcal{G}(k_F, i\omega; \pi) - \mathcal{G}(k_F, i\omega; 0)$ can be written (say, for Im $i\omega > 0$) as $E_F^{-\alpha}(i\omega)^{\alpha-1} g\left[t_\perp E_F^{-\alpha}(i\omega)^{\alpha-1}\right]$, where $g[x]$ is a *scaling* function. The change of variables $\omega = x\ {t_\perp}^{1/(1-\alpha)}$ gives $\Delta n_{k_F} \propto (t_\perp/E_F)^{\alpha/(1-\alpha)}$ times a dimensionless integral, which converges at large x for $\alpha < 1/2$. To assure convergence at low frequencies it is essential to expand the *self-energy* (Γ^{-1}) in $t_\perp$ and not directly the Green's function, in order to avoid an *unphysical* low-frequency (or low-T) divergence. For $\alpha > 1/2$ the integral diverges for large x and one needs to introduce a large-energy cutoff yielding a dominant linear behavior $\Delta n_{k_F} \propto t_\perp/E_F$. The same exponents would have been obtained by simply using the SDA for Γ. Notice also that this result is consistent with the one in Ref. [4].

In the $\alpha > \alpha_{2p}$ regime, one cannot straightforwardly extend the above discussion since the diagrams give non-homogeneous contributions. If one stops the expansion in $t_\perp$ for the *self-energy* at an arbitrary finite order ${t_\perp}^{m_0+1}$ one obtains (restricting to dominant terms at each order)

$$\mathcal{G}(k_F, i\omega; \pi)^{-1} \quad (3)$$
$$= t_\perp \sum_{m=-1}^{m_0} a_m \left((i\omega)^{\alpha-1} E_F^{-\alpha} t_\perp\right)^m \left(\frac{i\omega}{E_F}\right)^{(1-B)[m]_4} ,$$

where $[m]_4$ is defined as $4\ \mathrm{int}((m-2)/4) + 2$, int being the (lower) integer part, and the a_m are constants ($a_0 = 1$) possibly dependent on the spin and charge velocities. $\mathcal{G}(k_F, i\omega; 0)^{-1}$ is obtained from the same expression by replacing $t_\perp \to -t_\perp$. By inserting (3) into the integral (2) one can show that the integral is dominated by the constant and by the ${t_\perp}^{\overline{m}_0+1}$ terms in (3). Carrying out the integral yields $\Delta n_{k_F} \propto {t_\perp}^{R[\overline{m}_0]}$, where the exponent $R[\overline{m}_0]$ approaches quite rapidly its $\overline{m}_0 \to \infty$ limit $R = \alpha/(B-\alpha)$. For $R > 1$ this term will again be shaded by the linear term as in the case $\alpha < \alpha_{2p}$. In Fig. 2, we show the *dominant* and some subdominant exponents for the spinless and spinful cases as a function of α. As one can see, the occurrence of the two-particle regime ($\alpha > \alpha_{2p}$) reduces the dominant exponent in the spinless case, and, in particular, it shifts upwards (from $\alpha > 1/2$ to $\alpha > 2/3$) the region where Δn_{k_F} becomes linear in $t_\perp$. It is interesting to compare this result with the prediction of linear-response theory, which is expected, for sufficiently small $t_\perp$, either to give the correct behavior or to diverge thus signaling a sublinear behavior. The linear-response result $\Delta n_k = t_\perp(A + B|k_\parallel - k_F|^{2\alpha-1})$ indeed shows a divergence at $k_\parallel = k_F$ for $\alpha < 1/2$, i. e. it predicts a sublinear behavior in this region. However, our calculation shows that in the spinless case Δn_{k_F} is sublinear in $t_\perp$ in a *larger* region, namely, up to $\alpha = 2/3$. Unfortunately, this effect is more difficult to see in the case of electrons with spin, since in this case $\alpha_{2p} \approx 0.62 > 1/2$ and the effect is "shaded" by the linear behavior occurring for $\alpha > 1/2$. Nevertheless, this effect should be detectable, e.g., in the first derivative of Δn_{k_F} with respect to k or in the FS warp as discussed below. Notice that the exponent R has been obtained by cutting the series in $t_\perp$ *for the self-energy* Γ^{-1} at a given order. For $\alpha > \alpha_{2p}$, a different choice, like, e.g., cutting the series *for* Γ, may lead to a different (although in this case unphysical) result, which, however, preserves the qualitative effects, in particular the decrease of the exponent R. It should be mentioned that recently S. Capponi, D. Poilblanc and myself [12], have evaluated the exponent of Δn_{k_F} by exact diagonalization of small ladders supplemented by a careful finite-size extrapolation carried out by means of an appropriate scaling function. These numerical results are in very good accordance with the exponents for Δn_{k_F} predicted here and clearly show the change of behavior between the two regimes $\alpha < \alpha_{2p}$ and $\alpha > \alpha_{2p}$.

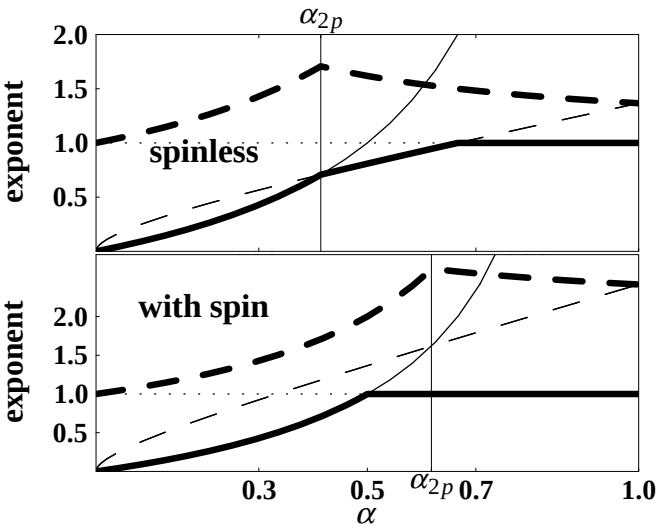

FIG. 2. Exponents controlling the behavior as a function of $t_\perp$ of Δn_{k_F} (thick solid line), and of the FS warp Δk_F (thick dashed line) for the N-chains system. Thin lines indicate subdominant exponents for Δn_{k_F} : $\alpha/(1-\alpha)$ (solid), $\alpha/(B-\alpha)$ (dashed), and unity (dotted). The exponents are plotted as a function of the correlation exponent α for the spinless and for the spinful cases.

We now study the behavior of the Fermi surface

as a function of $t_\perp$. The FS consists of the points $k_{\parallel F}[k_\perp]$ given by the solution of the equation [10] Re $\mathcal{G}(k_{\parallel F}[k_\perp], i\omega = 0^+; k_\perp)^{-1} = 0$. As already discussed [2,5,8], within the SDA a solution exists and gives $k_{\parallel F}[k_\perp] - k_F \propto |t_\perp[k_\perp]|^{1/(1-\alpha)}$. At higher order, $\mathcal{G}(k_\parallel, i\omega = 0^+; \pi)^{-1}$ has the same form as (3) with $i\omega$ replaced with $k_\parallel - k_F$ and with different coefficients a_n, whereby B is formally replaced with 1 for $\alpha < \alpha_{2p}$. The equation for the $(k_\perp = \pi)$ pole can be written in terms of a scaling function f as $f[t_\perp/(k_\parallel - k_F)^{1-\alpha}] = 0$. If $f[x] = 0$ has a solution at some point $x = x^*$, then the behavior of the FS is similar to the one for the SDA, i.e. $\Delta k_F \equiv k_{\parallel F}[\pi] - k_{\parallel F}[0] = (t_\perp/x^*)^{1/(1-\alpha)}$ [16]. This quantity measures the FS warp produced by $t_\perp$. However, it is not easy to find out whether the imaginary part of $\mathcal{G}^{-1}$ vanishes fast enough at the FS, so that the above result does not necessarily imply that the system goes into a Fermi liquid state. Moreover, considering higher-order terms for $f[x]$, the solution of $f[x] = 0$ may not exist. In fact, several gaps open in the different modes of a N-chain system [17], which could possibly prevent the pole equation from having a solution for some N and some $k_\perp$ points of the FS. In this case, as a measure of the FS warp, one could define a "pseudo" FS by the point $k_\parallel$ for which $|\mathcal{G}^{-1}|$ has a minimum. Also in this case, the FS warp turns out to behave like ${t_\perp}^{1/(1-\alpha)}$. Finally, for $\alpha > \alpha_{2p}$ the behavior for small $t_\perp$ is again dominated by the dot diagram (α) and by the higher-order diagrams of type γ and δ, as for the calculation of Δn_{k_F} . In a similar way, one obtains for the FS warp $\Delta k_F \propto {t_\perp}^{R/\alpha}$ (cf. Fig. 2). This means that the Fermi surface is warped even for $\alpha \to 1$ in contrast with the SDA result and with the expectation coming form the fact that $t_\perp$ is "irrelevant" for $\alpha > 1$. Notice, however, that particle-hole instabilities producing a gap at the Fermi surface are likely to occur for large α.

In conclusion, using a diagrammatic representation of the expansion in power of $t_\perp$, we have determined the power-law behavior as a function of $t_\perp$ of the difference in occupation Δn_{k_F} and of the FS warp in a N-chain system, our results being exact at *any finite order* for the self-energy. In the single-particle regime ($\alpha < \alpha_{2p}$), the exponents are correctly given by the low-order approximations. In the two-particle regime ($\alpha > \alpha_{2p}$) higher-order diagrams give dominant contributions and reduce the exponents (thus indicating an increased coherence) with respect to the SDA result. In this regime, linear-response theory in $t_\perp$ is not reliable *even in the small-$t_\perp$* limit. The increase of the exponents with α, as seen in Fig. 2, shows that transverse coherence is reduced with increasing interaction but never completely suppressed since Δn_{k_F} and the Fermi surface warp are finite for any finite value of $t_\perp$ also for large α. We expect, however, that at some value of α, a gap opens due to particle-hole instabilities possibly producing incoherence effects in the intrachain transport. For a finite number of chains these gaps seems to open even for small α [17]. It would be interesting to establish whether a finite critical value of α exists in the $N \to \infty$ limit.

I'm grateful to J. Voit for stimulating my interest in the topic of quasi-one-dimensional systems. I also acknowledge many interesting and fruitful discussions with M. G. Zacher, S. Capponi, D. Poilblanc, B. Brendel, G. Hildebrand and W. Hanke. This work was supported by the EC-TMR program ERBFMBICT950048.

[1] L. P. Gor'kov and I. E. Dzyaloshinskii, Sov. Phys. JETP **40**, 198 (1974); D. G. Clarke, S. P. Strong, and P. W. Anderson, Phys. Rev. Lett. **72**, 3218 (1994).
[2] X. G. Wen, Phys. Rev. B **42**, 6623 (1990).
[3] H. J. Schulz, Int. J. Mod. Phys. **5**, 57 (1991).
[4] C. Castellani, C. Di Castro, and W. Metzner, Phys. Rev. Lett. **69**, 1703 (1992); *ibidem* **72**, 316 (1994).
[5] D. Boies, C. Bourbonnais, and A.-M. S. Tremblay, Phys. Rev. Lett. **74**, 968 (1995).
[6] D. Clarke and S. Strong, J. Phys. Cond. Matt. **9**, 3853 (1997).
[7] A. Houghton and J. B. Marston, Phys. Rev. B **48**, 7790 (1993); P. Kopietz, V. Meden, and K. Schönhammer, Phys. Rev. Lett. **74**, 2997 (1995).
[8] K. Schönhammer, cond-mat/9710343; A. M. Tsvelik, cond-mat/9607209.
[9] S. A. Brazovskii and V. M. Yakovenko, Sov. Phys. JETP **62**, 1340 (1985).
[10] Throughout this paper, we use the conventions of Ref. [18] for the correlation exponents α and K_ρ, and restrict to $\alpha, K_\rho < 1$. Moreover, we set the *non-interacting* Fermi velocity $v_F = 1$ and the chemical potential $\mu = 0$. k_F indicates the Fermi momentum of the $t_\perp = 0$ system.
[11] W. Metzner, Phys. Rev. B **43**, 8589 (1991).
[12] S. Capponi, D. Poilblanc, and E. Arrigoni, Phys. Rev. B (98) *in press* (cond-mat/9709169),
[13] Notice that in this case one has a special Fermi liquid since the imaginary part of the self energy is *identically* zero in a finite region around $k_{\parallel F}[k_\perp]$.
[14] For definiteness, we consider the right-moving branch with external index $r = +$.
[15] Here, Γ is expressed in real space and imaginary time for the interchain coordinates $\mathbf{x} \equiv (x, i\tau)$ and in momentum space for the intrachain coordinate. For simplicity, we will set the spin and charge velocities equal to v_F $(= 1)$. This does not change the scaling behavior we are considering. In the following, the index S equals 1 (2) in the spinless (spinful) case, $a \propto E_F^{-1}$ is a short-distance cutoff, and $T = 0$. Moreover, we take N even and restrict t_{ij} to nearest neighbors. Notice that the -1 in square brackets in Eq. (1) comes from the disconnected part that has to be subtracted in order to obtain the cumulant C_4^0. This term is important otherwise the integral would diverge in the infinite-volume limit.
[16] Here, we used the symmetry $k_{\parallel F}[0] = 2k_F - k_{\parallel F}[\pi]$.
[17] See, e.g. H.-H. Lin, L. Balents, and M. P. Fisher, Phys. Rev. B *in press*, (1997), (cond-mat/9703055).
[18] J. Voit, Reports on Progress in Physics **58**, 977 (1995).